THE ASTROPHYSICAL JOURNAL, 545:L47–L51, 2000 December 10

A LACK OF PLANETS IN 47 TUCANAE FROM A *HUBBLE SPACE TELESCOPE* SEARCH[1]

RONALD L. GILLILAND,[2] T. M. BROWN,[3] P. GUHATHAKURTA,[4] A. SARAJEDINI,[5] E. F. MILONE,[6] M. D. ALBROW,[2]
N. R. BALIBER,[7] H. BRUNTT,[8] A. BURROWS,[9] D. CHARBONNEAU,[3,10] P. CHOI,[4] W. D. COCHRAN,[7]
P. D. EDMONDS,[10] S. FRANDSEN,[8] J. H. HOWELL,[4] D. N. C. LIN,[4] G. W. MARCY,[11] M. MAYOR,[12]
D. NAEF,[12] S. SIGURDSSON,[13] C. R. STAGG,[6] D. A. VANDENBERG,[14]
S. S. VOGT,[4] AND M. D. WILLIAMS[6]

Received 2000 August 25; accepted 2000 October 10; published 2000 November 28

ABSTRACT

We report results from a large *Hubble Space Telescope* project to observe a significant (~34,000) ensemble of main-sequence stars in the globular cluster 47 Tucanae with a goal of defining the frequency of inner orbit, gas giant planets. Simulations based on the characteristics of the 8.3 days of time series data in the F555W and F814W Wide Field Planetary Camera 2 (WFPC2) filters show that ~17 planets should be detected by photometric transit signals if the frequency of hot Jupiters found in the solar neighborhood is assumed to hold for 47 Tuc. The experiment provided high-quality data sufficient to detect planets. A full analysis of these WFPC2 data reveals ~75 variables, but no light curves resulted for which a convincing interpretation as a planet could be made. The planet frequency in 47 Tuc is at least an order of magnitude below that for the solar neighborhood. The cause of the absence of close-in planets in 47 Tuc is not yet known; presumably the low metallicity and/or crowding of 47 Tuc interfered with planet formation, with orbital evolution to close-in positions, or with planet survival.

Subject headings: binaries: eclipsing — globular clusters: individual (NGC 104, 47 Tucanae) — planetary systems — techniques: photometric

1. INTRODUCTION

The discovery of 51 Peg b (Mayor & Queloz 1995) in a remarkably tight orbit of 4.2 days around its Sun-like host star challenged prevailing theoretical views and impelled rapid progress in expanded radial velocity (RV) surveys that have now resulted in about 50 planet detections (see recent review by Marcy, Cochran, & Mayor 2000). The existence of inner orbit, gas giant planets (hot Jupiters) enables a highly efficient photometric search for planets, since with tight orbits (0.04–0.05 AU) hot Jupiters present about a 10% chance of transiting the host star given random orbital inclinations. Indeed, the transiting planet of HD 209458 was observed (Charbonneau et al. 2000; Henry et al. 2000) "on schedule," just as the ensemble of RV-detected hot Jupiters neared the point of a 50% expectation for transits. HD 209458b verified the theory of Guillot et al. (1996) predicting somewhat extended radii of ~1.2–1.4 R_J as a result of retarded cooling due to high irradiance from the host star. A transit depth of 1.7% and a duration of 3.0 hr for HD 209458b repeating every 3.525 days present an enticing photometric signal.

In 1998 when the number of detected extrasolar planets was ~10, of which four were hot Jupiters (defined herein as $P_{\rm orb} <$ 5 days), we proposed (in the "scientifically risky" category) to use the Wide Field Planetary Camera 2 (WFPC2) on the *Hubble Space Telescope* (*HST*) to observe a large ensemble of stars in 47 Tuc. Our target was selected (1) to provide an ideal spatial and brightness distribution of stars matching *HST* capabilities and (2) to shed insight into understanding the origins of planets by observing a system with reduced metallicity [Fe/H] = -0.7, [α/Fe] = 0.4 dex (Salaris & Weiss 1998). Our proposed field, with the crowded core of 47 Tuc on the PC1 CCD of WFPC2, provides some 40,000 main-sequence targets [giants are not of interest since the transit depth is equal to $(R_P/R_*)^2$, where R_P and R_* are the planet and star radii, respectively]. Saturation on the bright end occurs near the cluster turnoff where stellar radii are rapidly increasing and thus the expected signal is dropping anyway. Stars far down (~4 mag) the main sequence remain viable targets since a rising signal from falling stellar radii would balance declining signal-to-noise ratio (S/N) for these fainter stars. The frequency of hot Jupiters (nine are now known) in the solar neighborhood is about 1%, with about a 10% chance per system of random orbital inclinations yielding transits; the 47 Tuc ensemble should thus provide on the order of one planet per 1000 surveyed stars.

2. OBSERVATIONS

To detect two consecutive transits requires an observing interval twice the orbital period with continuous (relative to

[1] Based on observations with the NASA/ESA *Hubble Space Telescope* obtained at STScI, which is operated by AURA, Inc., under NASA contract NAS5-26555.

[2] Space Telescope Science Institute, 3700 San Martin Drive, Baltimore, MD 21218; gillil@stsci.edu.
[3] High Altitude Observatory, National Center for Atmospheric Research, P.O. Box 3000, Boulder, CO 80307; NCAR is sponsored by the National Science Foundation.
[4] UCO/Lick Observatory, University of California at Santa Cruz, Santa Cruz, CA 95064.
[5] Astronomy Department, Wesleyan University, Middletown, CT 06459.
[6] Physics and Astronomy Department, University of Calgary, Calgary, T2N 1N4, Canada.
[7] Department of Astronomy, University of Texas at Austin, Austin, TX 78712.
[8] Institute for Physics and Astronomy, Aarhus University, DK-8000, Aarhus C, Denmark.
[9] Department of Astronomy, University of Arizona, 933 North Cherry Avenue, Tucson, AZ 85721.
[10] Harvard-Smithsonian Center for Astrophysics, 60 Garden Street, Cambridge, MA 02138.
[11] Department of Astronomy, University of California, Berkeley, 601 Campbell Hall, Berkeley, CA 94720.
[12] Observatoire de Genève, CH-1290 Sauverny, Switzerland.
[13] Department of Astronomy, Pennsylvania State University, 525 Davey Laboratory, University Park, PA 16802.
[14] Department of Physics and Astronomy, University of Victoria, Victoria, BC, V8W 3P6, Canada.

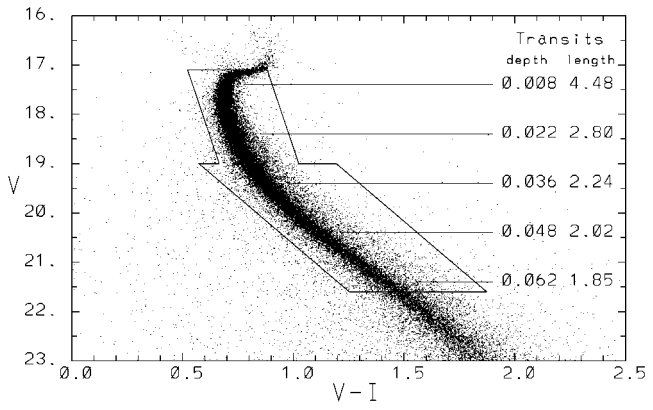

FIG. 1.—Color-magnitude diagram of 46,422 stars from all four WFPC2 CCDs. The box along the main sequence over $17.1 < V < 21.6$ shows the selection domain for the 34,091 stars reported herein (PC1 box extended to $V = 16.1$). Numerical entries provide predicted transit depths in magnitudes and duration (central passage) in hours assuming a $P_{\rm orb} = 3.8$ day planet with $R = 1.3\ R_{\rm J}$.

~2–3 hr transit timescale) coverage. Our 8.3 days (120 orbits of *HST*, GO-8267) of continuous observation spanned 1999 July 3–11, the only data gaps resulting from Earth occultations and passages through the South Atlantic Anomaly (SAA). We chose the F555W and F814W filters for the primary time series with 160 s exposures (cycled every 4 minutes in each), yielding saturation near $V \sim 17.1$ at cluster turnoff. These two filters were alternated in a sequence typically consisting of 6 × F555W and 6 × F814W during each SAA free orbit. Visibility periods impacted by the SAA were alternately devoted to one or the other filter. With the orbital period of *HST* of ~96.4 minutes, each transiting system of interest should display at least two consecutive transits over the 8.3 days in each of two filters. (Transits should be gray, while chance superposition of a main-sequence star and a large-amplitude but faint eclipsing binary, which in superposition mimics a planet transit in depth, would display very red signals.) The number of 160 s exposures obtained was 636 for F555W and 653 for F814W. We took care to design the observations with significant margin such that minor changes in one or even several assumptions regarding number of stars, realized photometric precision, planet radius and hence signal amplitude, or assumed frequency of systems would not jeopardize a robust result.

The primary consideration in detection margin is the ratio of signal amplitude to the time series precision multiplied by (for Gaussian noise) the square root of the number of data points during transits. Time series precisions reach nearly the Poisson limit, e.g., at $V = 18.4$ in 160 s an S/N of 200 (or 0.0053 mag rms) results in the F555W filter. The length of transits (including reduction by $\pi/4$ for average chord lengths) in hours (geometry plus Kepler's third law) and probability in percent of transits per existing system given random inclinations are

$$\tau_{\rm tran} = 1.412 M_*^{-1/3} R_* P_{\rm orb}^{1/3},$$
$$\Pr_{\rm tran} = 23.8 M_*^{-1/3} R_* P_{\rm orb}^{-2/3}, \quad (1)$$

where M_* and R_* are in solar units and $P_{\rm orb}$ is in days. For a 47 Tuc star at $V = 18.4$, $M_* = 0.81$, and $R_* = 0.92$ (Bergbusch & Vandenberg 1992), $\tau_{\rm tran} = 2.20$ hr (up to 2.80 for central passages) for $P_{\rm orb} = 3.8$ days and $\Pr_{\rm tran} = 9.6\%$. The transit depth (assuming $R_P = 1.3\ R_{\rm J}$) is predicted to be 0.022 (about 4 σ per observation), yielding an 11.5 σ detection per transit per filter. Overall this example would provide about a 23 σ detection.

3. ANALYSES AND TIME SERIES EXAMPLES

Full discussion of the analysis steps will appear in R. L. Gilliland et al. (2000, in preparation); here we provide only a sketch of steps relevant to reaching Poisson noise–limited results for undersampled, dithered, crowded field photometry with the added complication of frame-to-frame focus drift. We do not believe that any software packages previously described in the literature would be up to the specialized and stringent requirements of this project and have therefore developed our own procedures and codes. Gilliland et al. (1995) discuss issues relevant to precise time series photometry for undersampled and dithered *HST* data; the steps to robust cosmic-ray elimination using a polynomial expansion of the detected intensity as a function of (x, y) offsets to create an oversampled mean model remain central to the processing (for further details see Gilliland, Nugent, & Phillips 1999).

Initial frame-to-frame offsets are determined by point-spread function (PSF) fits to four relatively isolated stars in each frame. For each pixel a "surface" fit of intensity as a function of subpixel (x, y) offsets is formed with iterative elimination of multisigma positive deviations (cosmic rays). The frame-to-frame offsets are then adjusted by solving for the (x, y) offsets in a least-squares sense that provide a best match for evaluation of the analytic model (using only pixels on bright, unsaturated stars) to each frame. The image model and registration (including plate scale changes) solution are iterated two or three times to convergence.

Absolute photometry has been performed on four oversampled, co-added images using DAOPHOT II (Stetson 1992). A typical PSF FWHM is 1.4 pixels; PC and WF CCD plate scales are 0.″046 and 0.″1 per direct pixel, respectively. Figure 1 shows the color-magnitude diagram (CMD) of 47 Tuc developed from our deep, well-dithered, co-added images in F555W (101,760 s) and F814W (104,480 s). Zero points of the instrumental magnitudes have been adjusted to best match 47 Tuc *V*, *I* fiducials (Kaluzny et al. 1998) near main-sequence turnoff. Stars have been excluded if (1) nominal apertures (69 pixel PC, 45 pixel WF) touch saturated pixels from neighbors, (2) apertures include any bad pixels flagged in the data quality files (except saturation), (3) greater than 90% of the light in the aperture comes from wings of brighter nearby neighbors, or (4) more than 1% of the frames in both F555W and F814W show saturation in the core (gain = $14e^-$ DN^{-1}). For the results discussed further below only the 34,091 stars falling within a bright main-sequence box as shown were analyzed for time series.

The state-of-the-art crowded field, time series photometry now involves creation of difference images (e.g., Alcock et al. 1999; Alard 1999), where for well-sampled, ground-based CCD data excellent gains over classical PSF fitting in direct images are realized. With good difference images nonvariable objects are removed (except for residual, unavoidable Poisson noise), leaving any variables clearly present as isolated (positive or negative) PSFs even if the variable was badly blended with brighter stars in the direct images. Extraction of precise relative photometry changes for any star in a difference image can be handled with either aperture photometry or PSF fitting, and precise knowledge of the PSF is much less critical for the difference images relative to attempting photometry on blended stars in the direct image.

Difference images were created for each individual frame

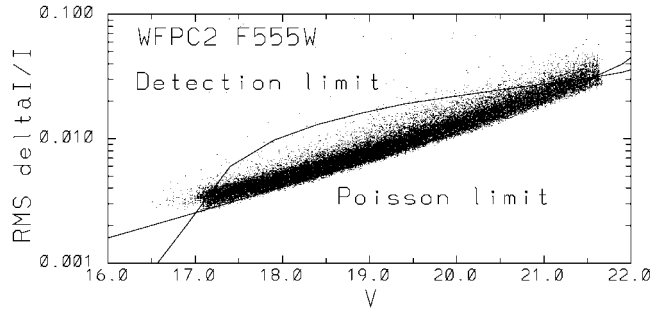

FIG. 2.—Final time series quality shown as standard deviation of intensity changes divided by the mean intensity for each star in the WFPC2 F555W bandpass. The lower curve defines the expected precision limit based on Poisson noise for isolated stars and background plus readout noise. Deviations to higher values usually follow from either real variables or increased (background) Poisson noise from near neighbors. The upper detection limit curve defines the line below which transits are predicted to provide greater than 6.5 σ detection for two transits in each filter; at this threshold no false alarms should arise.

using the intensity of the (x, y) analytic model evaluated at the position of each individual frame. Such images, however, showed large residuals at each star in many images as a result of focus changes. The 2 μm "breathing" of *HST* due to changing thermal stresses over orbits leads to a full amplitude redistribution of light inside to outside of a 1 pixel radius of ~20%. We have added the extra step of solving for a compensation kernel such that when convolved onto the analytic $I(x, y)$ model it best matches individual frames. An iteration is now adopted over this focus compensation, the registration solution, and the (x, y) intensity analytic model. Difference images can now be formed accounting for (x, y) offsets and focus changes; variable stars become obvious in movies of such images that were invisible in direct image movies.

A time series was created by fitting a PSF at the known position of individual stars in each image. Normalization was performed using counts as a function of magnitude based on archival calibration images of the standard GRW +70D5824. Each time series was cleaned by removing any changes linearly correlated with an ensemble average term and nine vectors comprising all terms through cubic in (x, y) offsets. This decorrelation step usually does not provide much change for the inherently excellent *HST* time series.

Figure 2 shows the resulting time series rms of relative intensities (magnitudes would be larger by a factor of 1.086) for each of 34,091 stars in the F555W filter (F814W results are similar). The lower curve shows the ideal photometry limit: our results are usually within ~10%–15% of this. The upper "detection limit" curve is a function of assumed planet radius, stellar radius along the main sequence, length of transits, and density of sampling such that a (Gaussian noise) rms value falling below this curve would provide greater than 6.5 σ detection for two transits in each filter. The steep dropoff of the detection capability on the bright end results from increasing stellar radii near turnoff, creating a lower predicted transit signal. At the faint end smaller stellar radii produce deeper but shorter transits, the S/N for which is overtaken by the loss in time series S/N in the sky background–limited regime.

Figure 3 shows a time series that presents a close approximation to expectations for a planet transit. The star has $V = 19.01$, $V-I = 0.89$, and two neighbors brighter by ~2.5 mag at 0.″5 separation. Decreases of ~3% can be seen repeating every 1.34 days in both the direct *V*- and *I*-band time series

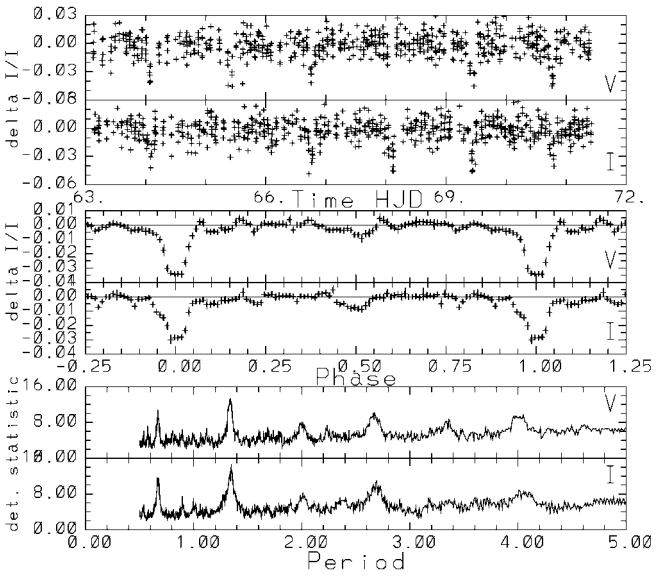

FIG. 3.—*Top panels:* Direct *V* and *I* light curves. *Middle panels:* Same as top panels, but phased at 1.340 days after smoothing over 0.036 bins (error bars show standard error from scatter within bins). Transit depths are as expected for a 1.3 R_J planet and 0.77 $R_\odot$ star. This demonstrates excellent sensitivity to transits; however, as discussed in the text, this is a diluted eclipsing binary signal, not a planet. *Bottom panels:* Transit detection statistic described in § 4.

(a combined 28 σ detection). Predicted transit depths from a planet at 1.3 R_J are 0.030 as seen. A 4 σ significant secondary eclipse at phase 0.5 suffices for arguing that this is not a planet. Moreover, analysis of the saturated neighboring stars shows that one is a large-amplitude eclipsing binary at the same period and phase. The light curve plotted results from the eclipsing binary PSF wings at the position of the faint star, providing a diluted signal of an ordinary variable; this is not a planet candidate.

4. TRANSIT SEARCH AND DETECTION EFFICIENCY

To search for multiple transits, we fold the time series of each individual star in each filter with sufficient trial phases and periods within 0.5–8.3 days to densely cover phase space. We then convolve the folded time series with the theoretical light curve corresponding to nominal transits. The convolution is normalized so that, for a white-noise input, the convolution values are normally distributed with unit variance. Possible transits are indicated by period-phase combinations with large positive values of the convolution (see Fig. 3). Since the noise in the *HST* data is close to white, we selected a threshold of 6.3 σ, which should yield $\lesssim$1 false alarm for the entire search space given Gaussian statistics (e.g., Bevington 1969). A detailed description of procedures and results will appear in T. M. Brown et al. (2000, in preparation).

A key issue in interpreting detections (or lack thereof) is the efficiency with which real transits would be detected by our search algorithms. To estimate this efficiency, we inserted artificial transits into the data stream and processed the resulting modified data sets using the standard transit detection pipeline. These were blind tests, in which the analyst had no knowledge of the properties of the inserted transits nor of which stars were affected. One set of simulations inserted artificial transits by manipulating pixel values in the original images associated with 24 stars. By modifying the data at the image level, we verified

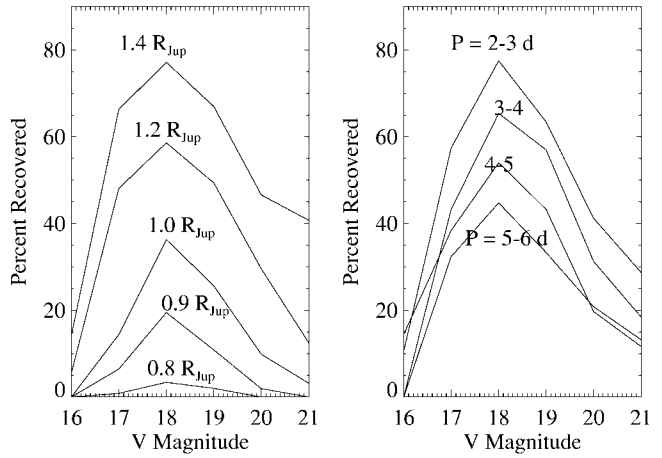

FIG. 4.—*Left panel:* Detection frequency averaged over periods from simulations as a function of assumed planet size. *Right panel:* Same as left panel, but as a function of orbital period at $R = 1.2\ R_J$.

that extensive image reduction and time series extraction steps used did not damage real transit signals. Our procedures correctly retained evidence of transits through the image processing and time series levels of the analysis.

A more extensive test inserted artificial transits directly into the time series of about 10,000 randomly chosen stars. These are enough samples to estimate the dependence of our detection efficiency on planetary radius and orbital period for the actual noise characteristics of our time series as a function of *V*. Figure 4 shows that the percentage of correctly categorized transit light curves depends strongly on assumed planet radius and more moderately on orbital period. The theoretical expectation (Guillot et al. 1996) is that (irradiated) planet radii vary only slowly as a function of mass. Indeed, planets with sub-Jovian mass may have slightly larger radii than a 1 M_J planet. Also, over the 2 orders of magnitude mass range from planets to brown dwarfs to stars at the main-sequence threshold, radii are not expected to vary by more than 10%–20%. This lack of radius dependence on mass would be a hindrance if trying to interpret a handful of weak signals as planets (rather than stars), but for a null result it implies a lack in the sample of any transiting planets, brown dwarfs, or very late M dwarfs.

Assuming an occurrence rate for close-in giant planets that is the same as in the solar neighborhood (0.8%–1.0%) and a 10% probability of favorable orbital alignment, there should be about 30 transiting planets among our sample of 34,091 stars. Assuming planet radii of 1.3 R_J and a typical period of 3.5 days and allowing for the actual distribution of *V* magnitudes (stellar radii and time series noise) in our sample, the number of planets actually detected should have been about 17. Since we saw none, we may conclude (with very high confidence) that in so far as giant planet occurrence is concerned, the solar neighborhood and 47 Tuc represent different populations.

5. ASTROPHYSICAL INTERPRETATION

It was noted (Gonzalez 1997) with the first planet detections that host stars tend to be considerably more metal rich than the average star surveyed in the solar neighborhood. This correlation has been maintained (Laughlin 2000) with a much larger sample now available. A correlation with metallicity could, however, be either cause or effect. It could be that lower metallicity in proto–planetary nebulae causes a lower frequency of planet formation as a result of fewer dust grains for nucleation. It could be that higher metallicity in systems with a remaining close-in planet is an effect of inward migration of metal-rich planets onto the star (Lin, Bodenheimer, & Richardson 1996), thus polluting the thin outer convective layer. Our 47 Tuc results are at least consistent with the hypothesis that lower metallicity biases against formation of hot Jupiters.

47 Tucanae is a massive cluster with a density $\sim 10^3\ M_\odot\ \mathrm{pc}^{-3}$ at 1′ from the core (Gebhardt & Fischer 1995; a typical location for our observations). In such a crowded environment, close encounters can result in dynamical interactions, particularly with passing binary systems, which lead to large changes in orbital parameters (Heggie 1975). Sigurdsson (1992) considered the orbital stability problem for high-mass ratio systems (in the context of pulsar planets) specifically for 47 Tuc conditions and concluded that orbits as short as 5 days would be quite stable against disruption or forced merger even in the most dense core region. An avenue for destroying hot Jupiters in the crowded 47 Tuc core arises from consideration of tidal dissipation (S. Sigurdsson, D. N. C. Lin, & R. L. Gilliland 2000, in preparation) within the planet. In this scenario star-planet encounters with binaries can induce an eccentric planet orbit. Dissipation of the stellar tidal disturbance within the planets drains their orbital energy. Internal heating may cause the planets to expand and provide positive feedback to a disruptive process. Critical to this scenario is the actual frequency of close binaries in 47 Tuc, which will be a valuable side product of our survey for planets (M. D. Albrow et al. 2000, in preparation). Alternative scenarios have been postulated where crowding limits planet formation (Armitage 2000).

We have shown that planets like 51 Peg b that are found in ~1% of local stars surveyed must be an order of magnitude rarer in the lower metallicity, crowded stellar environment extant in the center of 47 Tucanae. This represents a significant result delineating where planets exist. Further observations of stars in different circumstances will be necessary to learn whether the dominant influence in reducing the planet frequency is low metallicity, a crowded environment, or some combination of these or other factors.

We thank Merle Reinhart and Patricia Royle at STScI for assistance in scheduling these unique observations. This work was supported in part by STScI grant GO-8267.01-97A to the Space Telescope Science Institute and by several STScI grants from the same proposal to co-I institutions.

REFERENCES

Alard, C. 1999, A&A, 343, 10
Alcock, C., et al. 1999, ApJ, 521, 602
Armitage, P. J. 2000, A&A, submitted (astro-ph/0007044)
Bergbusch, P. A., & Vandenberg, D. A. 1992, ApJS, 81, 163
Bevington, P. R. 1969, in Data Reduction and Error Analysis in the Physical Sciences (New York: McGraw-Hill), 46
Charbonneau, D., Brown, T. M., Latham, D. W., & Mayor, M. 2000, ApJ, 529, L45
Gebhardt, K., & Fischer, P. 1995, AJ, 109, 209
Gilliland, R. L., Edmonds, P. D., Petro, L. D., Saha, A., & Shara, M. M. 1995, ApJ, 447, 191
Gilliland, R. L., Nugent, P. E., & Phillips, M. M. 1999, ApJ, 521, 30

Gonzalez, G. 1997, MNRAS, 285, 403
Guillot, R., Burrows, A., Hubbard, W. B., Lunine, J. I., & Sauman, D. 1996, ApJ, 459, L35
Heggie, D. C. 1975, MNRAS, 173, 729
Henry, G. W., Marcy, G. W., Butler, R. P., & Vogt, S. S. 2000, ApJ, 529, L41
Kaluzny, J., Wysocka, A., Stanek, K. Z., & Krzemiński, W. 1998, Acta Astron., 48, 439
Laughlin, G. 2000, ApJ, submitted (astro-ph/0008223)
Lin, D. N. C., Bodenheimer, P., & Richardson, D. C. 1996, Nature, 380, 606
Marcy, G. W., Cochran, W. D., & Mayor, M. 2000, in Protostars and Planets IV, ed. V. Mannings, A. P. Boss, & S. Russell (Tucson: Univ. Arizona Press), 1285
Mayor, M., & Queloz, D. 1995, Nature, 378, 355
Salaris, M., & Weiss, A. 1998, A&A, 335, 943
Sigurdsson, S. 1992, ApJ, 399, L95
Stetson, P. B. 1992, in ASP Conf. Ser. 25, Astronomical Data Analysis Software, ed. D. M. Worrall, C. Biemesderfer, & J. Barnes (San Francisco: ASP), 297